Soft Matter

PAPER

Cite this: *Soft Matter*, 2023, **19**, 276

Studying the high-rate deformation of soft materials *via* laser-induced membrane expansion†

Katherine M. Evans, Christopher L. Soles and Edwin P. Chan *

Received 21st October 2022,
Accepted 6th December 2022

DOI: 10.1039/d2sm01392d

rsc.li/soft-matter-journal

Cavitation is a phenomenon that occurs when the internal pressure of a material exceeds the resistance to deformation provided by the surrounding medium. Several measurements, such as the blister test, bubble inflation, and cavitation rheology, take advantage of this phenomenon to measure the local mechanical properties of soft materials at relatively low deformation rates. Here, we introduce a new measurement called laser-induced membrane expansion (LIME) that measures the shear modulus of a thin membrane at high strain rates ($\approx 10^6$ s^{-1} to 10^8 s^{-1}) by using laser ablation to rapidly expand a thin (tens of microns) elastomeric membrane. To demonstrate the capabilities of this measurement, we use LIME to study the mechanical properties of poly(dimethylsiloxane) (PDMS) membranes at several thicknesses (from 10 μm to 60 μm) and crosslink densities. We find that the shear modulus of the PDMS measured by LIME was weakly dependent on the crosslink density, but was strongly strain rate dependent with values ranging from 10^6 Pa to 10^8 Pa. This measurement platform presents a new approach to studying the mechanical properties of soft but thin materials over a range of deformation rates.

1 Introduction

From balloons to soap bubbles to foams and emulsions, cavitation is a common occurrence in everyday life. While it is a phenomenon that is often used to drive form and function, there have been significant efforts to leverage the expansion process of a bubble or cavity to quantify the mechanical properties of soft materials. These different cavitation-based measurement approaches, as a function of deformation rate, are summarized in Fig. 1(a). A classic measurement is the blister test. In this test, a thin membrane is draped over a small hole with the edges of the membrane clamped to form a free-standing membrane.[1–3] It is then inflated by pressurizing one side of the membrane, and the deformation of the membrane can then be used to quantify its mechanical properties, such as adhesion energy and elastic modulus. This test is a quasi-static test, with strain rates of 10^{-6} to 10^{-4} s^{-1}, and typically applied to thin membranes. Another test is the bubble inflation test, which dates back to the 1970s.[4–6] In this test, a cavity forms in a bulk material with the application of a pressurized gas. By measuring the cavity radius as a function of pressure, the mechanical properties, including elastic modulus and shear viscosity, can be determined. Large extensions are achieved, with typical strain rates spanning from 10^{-6} to 10^2 s^{-1}. A derivative of the bubble inflation test is nanobubble inflation, which measures the viscoelastic properties of ultrathin films.[7]

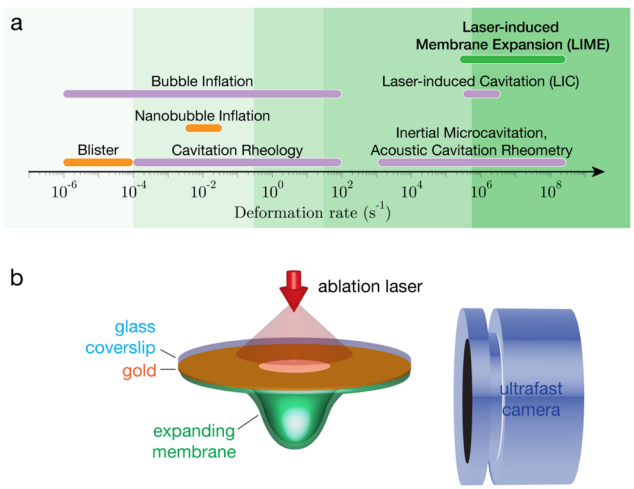

Fig. 1 (a) The different cavitation-based approaches for measuring the mechanical properties of soft materials at different deformation rates. (b) Schematic of the LIME experiment and ablation target.

There are more recent cavitation-based measurements that can study the mechanical properties of soft materials at higher strain rates. One such measurement is cavitation rheology,

Materials Science and Engineering Division, National Institute of Standards and Technology, 100 Bureau Dr, Gaithersburg, MD 20899, USA.
E-mail: edwin.chan@nist.gov; Tel: +1 301-975-5228

† Electronic supplementary information (ESI) available. See DOI: https://doi.org/10.1039/d2sm01392d

which relates the critical pressure required to grow a spherical bubble in a soft gel to its elastic modulus and surface energy.[8,9] The deformation rate of cavitation rheology can range from quasi-static (10^{-4} s^{-1}) to intermediate rates (10^{2} s^{-1}). A related technique, known as inertial microcavitation-based high strain rate rheometry, monitors the internal pressure of a cavity to quantify the elastic modulus.[10] As the name implies, this is a high strain rate test, with strain rates ranging from 10^{3} s^{-1} to 10^{8} s^{-1}. In this test, a laser or high-amplitude focused ultrasound is used to induce cavitation, and then the time-dependent oscillation of the bubble radius can be related to the viscoelastic properties of the material. A very recent development that is particularly relevant to this work is laser-induced cavitation (LIC).[11] In LIC, a laser-sensitive seed microparticle is intentionally ablated to nucleate and expand a cavity inside a bulk material. By measuring the radius of the bubble as a function of time, the shear modulus and viscosity can be determined. Similar to inertial microcavitation, this is also a high deformation rate test with rates on the order of 10^{6} s^{-1}. However, in LIC, the initial growth and decay process is measured to determine the material properties.

While these recent approaches are promising as they can study soft materials at high deformation rates, they have only been demonstrated to measure the mechanical properties of bulk materials. In this work, we present a new cavitation-based measurement approach that measures the high strain rate shear modulus of a thin elastomeric membrane, which we call laser-induced membrane expansion (LIME). We develop a scaling relationship relating the radius of the expanding bubble with the materials and experimental properties to show that the mechanism of the initial membrane expansion and subsequent retraction is a balance of three energies, (1) inertia of the membrane material, (2) the strain energy density of the elastomer, and (3) the blast energy initiated from the laser ablation process. We show that by controlling the thickness of the elastomeric membrane, LIME is able to achieve deformation rates from 10^{6} to 10^{8} s^{-1}. LIME is a promising measurement approach for measuring the mechanical properties of thin membranes at deformation rates over several orders of magnitude.

2 Results and discussion

2.1 LIME experiment

We developed LIME as an offshoot of laser-induced projectile impact testing (LIPIT), which uses a pulsed laser to cause propulsion of a microparticle at high velocities in the direction of the laser path.[12–14] Here, we use this concept of laser-based propulsion to drive the expansion of a polymer membrane in order to study its mechanical properties. A schematic of the LIME experiment is shown in Fig. 1(b). In this experiment, the laser absorptive material is prepared by first depositing a thin layer (≈30 nm) of gold onto a glass coverslip, which serves as the ablation target to facilitate membrane expansion. Next, we spin-coat the polymer film of interest onto the gold-coated cover slip. Crosslinked poly(dimethylsiloxane) (PDMS, Dow Corning Sylgard 184) was chosen as the material because it is a commonly used elastomer whose mechanical properties have been studied extensively. We note that PDMS is simply used as a representative material here, but we expect that other polymeric materials can be studied using LIME. To study the effect of elastic modulus on the membrane expansion process, three crosslink densities were studied here, 7.5 : 1, 15 : 1, and 30 : 1 denoting the composition of the base PDMS component to the crosslinking agent by mass. Additionally, the PDMS film thickness was also systematically varied between 10 μm and 60 μm.

A pulsed diode-pumped solid-state IR laser (Flare NX, wavelength = 1030 nm, pulse length = 1.5 ns, Coherent Inc.) was used as the ablation laser to ablate the gold layer. The laser power of ≈500 μJ was constant across all experiments conducted. The expansion of the PDMS membrane was monitored using an ultrafast camera (SIMD12, Specialized Imaging Ltd) with a frame rate of 10^{6} s^{-1}. Additional experimental details and parameters can be found in the ESI.†

Fig. 2(a) shows LIME data for a 10 μm thick 15 : 1 PDMS membrane. In frame 1, a bright spot can be seen at the top of the frame, which is from the plasma generated by the laser ablating the gold layer. Frames 2–5 show a rapid expansion of the membrane. Rather than forming a spherical cap, the shape of the membrane is more oblong. The oblong shape of the expanding PDMS membrane is most likely attributed to adhesive interactions between the peeling edge of the membrane and the substrate. This effect will be explored systematically in a follow-up work as it is an interesting way to study adhesion at fast deformation rates.

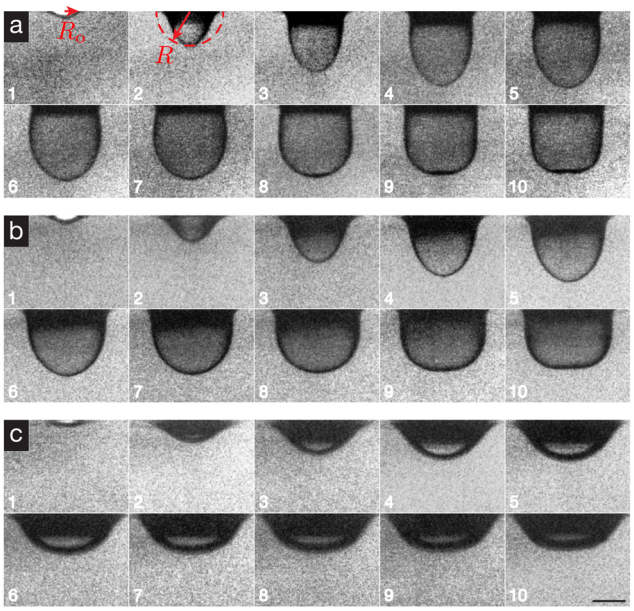

Fig. 2 LIME data for a 15 : 1 PDMS membrane with thickness and inter-frame time of (a) 10 μm/140 ns, (b) 35 μmm/140 ns, (c) 60 μmm/320 ns. Scale bar = 50 μm.

As a first-order approximation, we model the shape of the expanding membrane as a spherical cap, with the radius (R) defined in the vertical direction since the important metric is how far and fast the membrane expands away from the substrate (see Fig. 2(a), frame 2). The initial radius, R_o, is 25 μm for all experiments. It is defined by the initial spot size of the plasma from the laser ablation process and is independent of the properties of the PDMS membrane (see Fig. 2(a), frame 1). The stretch ratio, defined as $\lambda = R/R_o$, reaches a maximum of $\lambda_m = 9.0$ in frame 5. From frame 6 onwards, the membrane begins the slow retraction process. By frame 10, $\lambda = 7.9$, indicating that the retraction process is many times slower than the expansion process. Given the high λ_m reached, we expect there is permanent damage done to the PDMS membrane during the expansion process, but it is difficult to discern this from our LIME results. Fig. 2(b) and (c) show the LIME data for a 35 μm and a 60 μm thick 15 : 1 PDMS film, respectively. Qualitatively, they follow the same expansion process as the 10 μm thick film: plasma generation, followed by a rapid expansion of the membrane to a large stretch ratio, and finally, a slow retraction process. However, the membrane thickness does affect λ_m and the critical time to reach this maximum. The 10 μm thick film reaches $\lambda_m = 9.0$ at 700 ns. The 35 μm thick film reaches $\lambda_m = 4.2$ at 840 ns. The 60 μm film reaches $\lambda_m = 1.8$ at 1600 ns, which is five times lower in stretch and over two times slower compared to the thinnest membrane of the same PDMS formulation. Thus membrane thickness is a practical handle to control the rate of expansion and the extent of stretch.

Fig. 3 summarizes the radius (R) *versus* time (t) data for all the materials studied using LIME. The results show the observations quantitatively from the high-speed images. There is a very rapid increase in the radius at short times, followed by a plateau for a few hundred nanoseconds, and then a very slow retraction of the membrane. Due to the limited number of frames that can be captured by the camera and the slow retraction process, the entire membrane retraction process was not captured as we focused on the expansion process. Nevertheless, the effect of film thickness on λ_m and critical time to reach λ_m can be seen from Fig. 3. At a given crosslink density, we find that λ is shifted to longer times and reaches a lower λ_m with increasing membrane thickness. This is an important result since it shows that the kinetics of the expansion process is affected by the membrane thickness, which implies that the deformation rate ($\dot{\varepsilon}$) can be experimentally adjusted simply by changing membrane thickness. The crosslink density of the elastomer has a slight effect on the maximum radius of the expanded membrane. By and large, λ_m increases with decreasing crosslink density for a given film thickness. There are exceptions, such as for the 10 μm thick films, rendering the crosslink density a challenging parameter to use to control the stretch ratio. Additionally, the critical time to reach λ_m is quite similar for the same membrane thickness regardless of crosslink density.

2.2 Model for the inertial expansion of a membrane

To estimate the shear modulus of these membranes using the results in Fig. 3, we turn to prior studies of membrane expansion of soft materials to aid in the identification of the key parameters. A classic model for describing a high-rate and high-energy expansion process is Taylor's blast, which relates the radius of the shock front to time as,

$$R = \left(\frac{U}{\rho_m K}\right)^{1/5} t^{2/5} \quad (1)$$

where U is the energy of the blast, ρ_m is the density of air, and K is a dimensionless constant related to the thermal properties of air. This expression shows that the rate of shock wave expansion is governed by the energy input that drives expansion and is balanced by the density of air that impedes this expansion. This balance results in an inertia-dominated process, characterized by a time dependence of $R \sim t^{2/5}$.

Originally developed to relate the expansion rate of a shock front to the blast energy after a nuclear explosion,[15] it has since

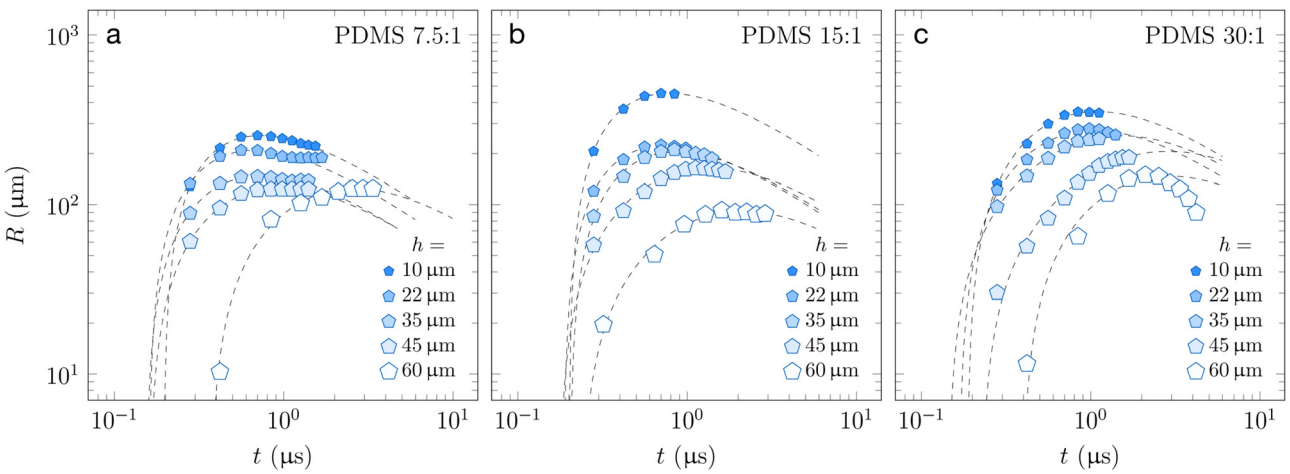

Fig. 3 Radius (R) *vs.* time (t) results for all of the LIME experiments on PDMS elastomers with crosslink ratio of (a) 7.5 : 1, (b) 15 : 1, (c) 30 : 1. Dotted lines are the fits from eqn (5). Error on the t is ±3 ns and error on R is ±6 μm.

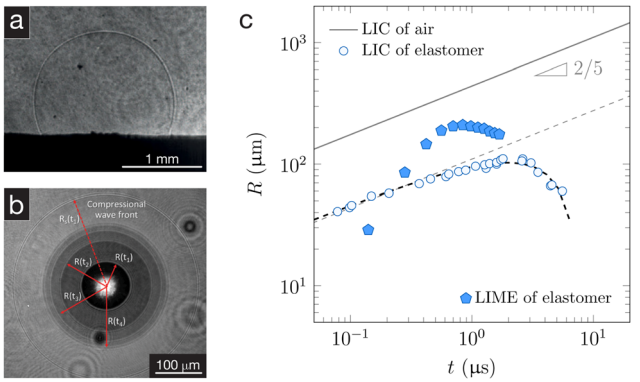

Fig. 4 Models of laser-induced expansion. (a) Laser ablation on a solid target in air, adapted from Chemin *et al.*,[16] and (b) laser-induced cavitation (LIC), adapted from Tiwari *et al.*[11] (c) Radius *versus* time data from LIC (open circles) and LIME (pentagons) showing the fit to LIC from eqn (2). The solid and dashed lines show the expected radius *versus* time curve for Taylor's blast, which scales as $R \sim t^{2/5}$. The black dashed line is a fit of the LIC data using eqn (2).

been adapted to fit other expansion processes, including laser-induced cavitation (LIC) of air.[16] Chemin *et al.* monitored the shock wave front that formed after laser ablation of a solid target in air and found that the change in radius of the shock front with time is consistent with the solution to Taylor's blast (Fig. 4(a)). In the case of LIC of air, U in eqn (1) is defined by the laser-ablation energy. Although the energy associated with LIC of air is many orders of magnitude lower compared to a nuclear blast, the kinetics of the shock wave follow the same scaling. Thus eqn (1) serves as an upper bound on how the radius of the membrane in a LIME experiment can be expected to change with time. Although both experiments use laser ablation, there is an additional constraint in LIME that alters the membrane expansion process.

Another experiment that studied the laser-induced expansion of soft materials is LIC of PDMS, discussed briefly in the introduction.[11] Here, a laser ablative seed microparticle was used to rapidly generate a cavity in a bulk sample of PDMS. The growth rate of the cavity is then related to the shear modulus and viscosity of the PDMS. This experiment is particularly relevant to LIME as both measurements use laser ablation to nucleate a cavity to expand an elastomer. The key difference between the two experiments is the geometry of the sample (bulk *vs.* membrane) and how the cavity is initiated (ablation seed *vs.* gold film). Nevertheless, the results between the two measurements share similarities.

We first discuss the results of the LIC of PDMS elastomers. Using the radius *vs.* time data extracted from LIC experiments of PDMS from Tiwari *et al.*,[11] we employ Buckingham Π dimensional analysis to develop a scaling relationship that relates the experimental parameters to the key materials properties. Full details on this analysis, as well as its relevance in other contexts, can be found in the ESI.† In brief, Buckingham Π is a type of dimensional analysis that can be used to generate dimensionless relationships even if the exact form of the expression is unknown.[17] In this analysis, all the relevant variables are identified and used to form the dimensionless Π groups. The relevant variables for both the LIC and LIME experiments are shown in Table 1.

Table 1 Experimental parameters and materials properties identified for LIME and LIC. Also included are the corresponding dimensions of these variables

Variable	Description	Dimensions	Test
R	Radius of expanding membrane	[L]	LIC, LIME
h	Membrane thickness	[L]	LIME
U	Laser ablation energy	$[ML^2/T^2]$	LIC, LIME
γ_{el}	Membrane tension	$[M/T^2]$	LIC, LIME
ρ_m	Surrounding medium density	$[M/L^3]$	LIME
ρ_p	Membrane density	$[M/L^3]$	LIC, LIME
t	Time	[T]	LIC, LIME

Using this methodology, we are able to generate a scaling relationship for the LIC of PDMS data from this analysis, shown in eqn (2),

$$R = c_1\left(\frac{U}{\rho_p}\right)^{1/5} t^{2/5} - c_2\left(\frac{\gamma_{el}}{U^{3/5}\rho_p^{2/5}}\right) t^{6/5} \quad (2)$$

where U is the energy of the laser, ρ_p is the density of the bulk PDMS elastomer, and c_1 and c_2 are proportionality constants with magnitudes ≈ 1. The parameter γ_{el} is a stiffness parameter that describes the elasticity of the expanding elastomer. Since this parameter is a function of λ and h, its exact form will depend on the specific material, which is discussed in the ESI† and below.

Eqn (2) has two terms. The first term has a time dependence of $t^{2/5}$ and should look familiar: this term is the same expression as the scaling relationship for Taylor's blast. Again, this first term relates the balance between the incident energy from the laser ablation event (U) causing the forward motion of the membrane and the inertia of the membrane defined by its density ρ_m. Since the membrane material has elasticity, the expansion is also constrained by membrane tension (γ_{el}), which is defined by the second term of eqn (2). Specifically, the second term is a balance between membrane tension *versus* the product of membrane density and blast energy and has a time dependence of $t^{6/5}$. The LIC data and the fit using eqn (2) are shown in Fig. 4(c). For the majority of the PDMS expansion process, LIC follows the same time dependence as Taylor's blast. It is only right before the cavity begins to contract that the radius of the cavity deviates from the prediction of eqn (1). This is an important observation because it shows that the expansion process is inertia dominated and the retraction process is membrane tension dominated.

From the insights given from Taylor's blast and LIC, we now apply this understanding to the LIME results. As mentioned previously, LIME shares similarities with LIC, albeit in a thin membrane geometry. We also apply Buckingham Π analysis to develop a scaling relationship, which is defined as,

$$R = c_4\left(\frac{\rho_m}{\rho_p}\right)^n\left(\frac{U}{\rho_p}\right)^{1/5} t^{2/5} - c_5\left(\frac{\gamma_{el}}{U^{2/5}\rho_p^{3/5}}\right) t^{6/5} - c_6 h \quad (3)$$

Full details on how the Buckingham Π analysis was conducted for LIC and LIME can be found in the ESI.† This relationship is similar to eqn (2), with a few important deviations. The first term is again Taylor's blast that describes the inertia-dominated expansion process at short times. However, there is an additional parameter in this term, which is the ratio of the density of the surrounding medium to the membrane density. This additional parameter is necessary to account for the fact that two separate materials (PDMS and air) are displaced during the expansion process. The second term is identical to that of eqn (2), which again describes the resistance of expansion due to membrane tension. The third term, which is unique to LIME, is a correction factor to account for the finite thickness of the membrane. It depends on h because it is another inertial term: there is a finite amount of material that must be displaced. This third term also suppresses the expansion process, which is observed from the results shown in Fig. 3. While eqn (2) and (3) are very similar, the modification of the second term due to γ_{el} and the addition of the third term cause deviation of the expansion process from Taylor's blast, as can be seen in Fig. 4(c).

The parameter γ_{el} is the membrane tension term that is a function of the shear modulus, stretch ratio, and film thickness. The exact form of the expression is material specific. Here, we choose the neo-Hookean model, for its simplicity with the fewest number of fitting parameters, to describe the nonlinear deformation of the PDMS elastomers. For a thin membrane, γ_{el} is defined as,

$$\gamma_{el} = \frac{h}{\lambda}\mu\left(\lambda^2 - \lambda^{-4}\right) \approx \frac{Rh}{R_o}\mu \tag{4}$$

Since the stretch ratio of the membranes is quite high ($\lambda \gg 1$), the λ^{-4} term is negligible, and the approximate functional form can be used. Substituting γ_{el} into eqn (3), the resulting expression is given by,

$$R = \frac{C_4 t^{2/5} - C_3 h}{1 + C_2(h/R_o)\mu t^{6/5}} \tag{5}$$

where μ is the shear modulus of the material, and C_2, C_3, C_4 are proportionality constants. We note that μ should more appropriately be defined as the complex shear modulus ($\mu^\star = \mu' + i\mu$), which takes into account elastic (μ') and viscous (μ'') effects that dominate at different deformation rates. For our current LIME experiments, where the strain rate is quite high, we expect that this complex shear modulus is primarily elastic.

2.3 Shear modulus measured *via* LIME

We use eqn (5) to fit the LIME results, and the fits are shown in Fig. 3. To determine the shear modulus of each individual membrane, the term in the denominator, $C_2(h/R_o)\mu$, was treated as a constant that was found from fitting the R *vs.* t data. Once that constant was determined, μ was then extracted by substituting the relevant membrane thickness for h and setting $R_o = 25$ μm and $C_2 \approx 1$. From Buckingham Π analysis, we know that C_2 is a proportionality constant that should be ≈ 1.

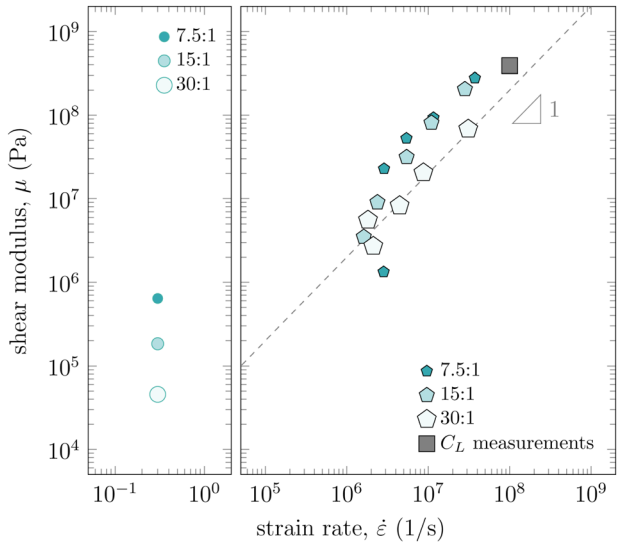

Fig. 5 Shear modulus of the PDMS elastomers as a function of strain rate and crosslink ratio measured using quasi-static tensile testing (circles) and LIME (pentagons). Also shown is the shear modulus value estimated from the acoustic wave speed (C_L) measurements separately reported by Veysset *et al.*,[20] and Lee *et al.*[21] For the study by Lee *et al.*, the PDMS elastomer crosslink ratio was 10 : 1.

The strain rate is estimated as $\dot{\varepsilon} = v_m/h$, where v_m is the initial velocity of the expanding membrane. Because it depends on membrane thickness, the strain rate inherently changes from sample to sample. Thus, not only can LIME determine the high strain rate shear modulus of the elastomer, we can also use it to characterize how the elasticity changes with strain rate by changing the membrane thickness. From Fig. 5, we find that the strain rate of our LIME experiments spans several orders of magnitude, ranging from 10^6 to 10^8 s^{-1}, resulting in a change in shear modulus of ≈2 MPa to ≈300 MPa. For comparison, we also measured the shear modulus of the same three PDMS systems under quasi-static uniaxial test conditions ($\dot{\varepsilon} = 0.3$ s^{-1}), and the results are also shown in Fig. 5. For PDMS elastomers at 7.5 : 1, 15 : 1, and 30 : 1 crosslink ratios, the shear moduli are 0.64 MPa, 0.18 MPa, and 0.046 MPa, respectively.

The shear modulus measured by LIME is much higher compared to the quasi-static values. However, this is not particularly surprising as strain rate stiffening is a well-known phenomenon in polymers that causes the mechanical properties, including the shear modulus, to change.[18,19] The increase in shear modulus as a function of strain rate may not be due only to strain rate stiffening. Prevalent in many high-rate deformation experiments, it is probable there is a temperature rise at the strain rates imposed by LIME due to adiabatic heating. Since elastomers can be modeled as entropic networks (*i.e.* rubber elasticity), an increase in temperature will lead to a proportional enhancement in the shear modulus of the PDMS elastomers. Both strain rate stiffening and temperature rise are plausible factors that contribute to the increase in shear modulus of the PDMS membranes seen here.

We also compared our results with acoustic wave speed studies of PDMS using LIPIT,[20] and Brillouin light scattering

(BLS).[21] In both studies, the authors were able to image or directly measure the longitudinal acoustic wave speed of the PDMS (C_L), which is related to its elastic modulus (E) and density, $E = \rho C_L^2$. Based on the estimated acoustic wave speed ($\approx$1.14 km s^{-1}) and PDMS density (ρ = 980 kg m^{-3}), we estimate that $\mu \approx 390$ MPa. As shown in Fig. 5, this value is consistent with our experiments.

Although the film thickness is paramount for controlling the shear modulus, we find that the crosslink density has very little effect. Under quasi-static conditions, the shear modulus of a 30 : 1 PDMS elastomer is $\approx 10\times$ less than the 7.5 : 1 PDMS elastomer. From the LIME results, we find that the shear modulus of the 7.5 : 1 and 15 : 1 elastomers are similar at a similar strain rate, and we estimate that $\mu \sim \dot{\varepsilon}$ for all three elastomer systems. Only the thinnest PDMS membranes with the lowest crosslink density (30 : 1) show a noticeable reduction in the shear modulus, but it is only approximately 3 $\times$ lower than the 7 : 5 and 15 : 1 elastomers. From the LIME experiment, it is unclear how the permanent crosslinks alone determine the elasticity of these materials. It is known that PDMS has both chemical crosslinks and physical entanglements. Under quasi-static conditions, the entanglements can potentially slip past each other, so the resistance to deformation is mostly attributed to the chemical crosslinks. However, the same entanglements likely do not have sufficient time to disentangle at high strain rates, and thus contribute to the elasticity of the elastomer.

3 Conclusion

In this work, we have developed a new technique, LIME, that can measure the high strain rate mechanical properties of polymer membranes. We developed a scaling relationship between the growth kinetics of an expanding membrane with the materials and experimental properties of the system, which allows us to extract the shear modulus of a polymer of interest. We demonstrated that the thickness of the film can be used to control the strain rate of expanding membrane, with strain rate varying between $\dot{\varepsilon} = 10^6$ to 10^8 s^{-1}. The high strain rate shear modulus of the PDMS elastomers was found to vary between 10^6 to 10^8 MPa depending on the strain rate. With the simplicity in sample preparation, along with the broad range of strain rates accessible by LIME, it opens up measurement opportunities for studying molecular effects such as dynamics of disentanglement in soft materials. Additionally, while not explored here, the range of strain rates achieved by LIME could potentially be expanded by changing the energy of the ablation process, which is something that we will explore in the future.

Conflicts of interest

Certain instruments and materials are identified in this paper to adequately specify the experimental details. Such identification does not imply recommendation by the National Institute of Standards and Technology; nor does it imply that the materials are necessarily the best available for the purpose.

Acknowledgements

This work is a contribution of NIST, an agency of the U.S. Government, and not subject to U.S. copyright.

Notes and references

1 X. Xu, C. Shearwood and K. Liao, *Thin Solid Films*, 2003, **424**, 115–119.
2 M. S. Islam and L. Tong, *Int. J. Adhes. Adhes.*, 2015, **62**, 107–123.
3 S. Guo, K.-T. Wan and D. A. Dillard, *Int. J. Solids Struct.*, 2005, **42**, 2771–2784.
4 D. D. Joye, G. W. Poehlein and C. D. Denson, *Trans. Soc. Rheol.*, 1972, **16**, 421–445.
5 D. D. Joye, G. W. Poehlein and C. D. Denson, *Trans. Soc. Rheol.*, 1973, **17**, 287–302.
6 Y. Li, J. A. Nemes and A. A. Derdouri, *Polym. Eng. Sci.*, 2001, **41**, 1399–1412.
7 P. A. OConnell and G. B. McKenna, *Rev. Sci. Instrum.*, 2007, **78**, 013901.
8 J. A. Zimberlin, N. Sanabria-delong, G. N. Tew and A. J. Crosby, *Soft Matter*, 2007, **3**, 763–767.
9 J. A. Zimberlin and A. J. Crosby, *J. Polym. Sci., Part B: Polym. Phys.*, 2010, **48**, 1423–1427.
10 J. B. Estrada, C. Barajas, D. L. Henann, E. Johnsen and C. Franck, *J. Mech. Phys. Solids*, 2018, **112**, 291–317.
11 S. Tiwari, A. Kazemi-Moridani, Y. Zheng, C. W. Barney, K. R. McLeod, C. E. Dougan, A. J. Crosby, G. N. Tew, S. R. Peyton, S. Cai and J.-H. Lee, *Soft Matter*, 2020, **16**, 9006–9013.
12 E. P. Chan, W. Xie, S. V. Orski, J.-H. Lee and C. L. Soles, *ACS Macro Lett.*, 2019, **8**, 806–811.
13 S. H. Chen, A. J. Souna, C. L. Soles, S. J. Stranick and E. P. Chan, *Soft Matter*, 2020, **16**, 3886–3890.
14 D. Veysset, J. H. Lee, M. Hassani, S. E. Kooi, E. L. Thomas and K. A. Nelson, *Appl. Phys. Rev.*, 2021, **8**.
15 G. I. Taylor, *Proc. R. Soc. London, Ser. A*, 1950, **201**, 159–174.
16 A. Chemin, M. W. Fawaz and D. Amans, *Appl. Surf. Sci.*, 2022, **574**, 151592.
17 E. Buckingham, *Phys. Rev.*, 1914, **4**, 345–376.
18 J. S. Bergström and M. C. Boyce, *J. Mech. Phys. Solids*, 1998, **46**, 931–954.
19 V. Kanyanta and A. Ivankovic, *J. Mech. Behav. Biomed. Mater.*, 2010, **3**, 51–62.
20 D. Veysset, A. J. Hsieh, S. Kooi, A. A. Maznev, K. A. Masser and K. A. Nelson, *Sci. Rep.*, 2016, **6**, 25577.
21 B. W. Lee, J.-H. Ko, J. Park, D.-M. Shin and Y.-H. Hwang, *J. Korean Phys. Soc.*, 2016, **68**, 896–900.